Location of brain lesions predicts conversion of clinically isolated syndromes to multiple sclerosis

Antonio Giorgio, MD
Marco Battaglini, PhD
Maria Assunta Rocca, MD
Alessandro De Leucio
Martina Absinta, MD
Ronald van Schijndel, PhD
Alex Rovira, MD
Mar Tintoré, MD
Declan Chard, MD
Olga Ciccarelli, MD
Christian Enzinger, MD
Claudio Gasperini, MD
Jette Frederiksen, MD
Massimo Filippi, MD
Frederik Barkhof, MD
Nicola De Stefano, MD
On behalf of the MAGNIMS Study Group

ABSTRACT

Objectives: To assess in a large population of patients with clinically isolated syndrome (CIS) the relevance of brain lesion location and frequency in predicting 1-year conversion to multiple sclerosis (MS).

Methods: In this multicenter, retrospective study, clinical and MRI data at onset and clinical follow-up at 1 year were collected for 1,165 patients with CIS. On T2-weighted MRI, we generated lesion probability maps of white matter (WM) lesion location and frequency. Voxelwise analyses were performed with a nonparametric permutation-based approach ($p < 0.05$, cluster-corrected).

Results: In CIS patients with hemispheric, multifocal, and brainstem/cerebellar onset, lesion probability map clusters were seen in clinically eloquent brain regions. Significant lesion clusters were not found in CIS patients with optic nerve and spinal cord onset. At 1 year, clinically definite MS developed in 26% of patients. The converting group, despite a greater baseline lesion load compared with the nonconverting group (7 ± 8.1 cm^3 vs 4.6 ± 6.7 cm^3, $p < 0.001$), showed less widespread lesion distribution (18% vs 25% of brain voxels occupied by lesions). High lesion frequency was found in the converting group in projection, association, and commissural WM tracts, with larger clusters being in the corpus callosum, corona radiata, and cingulum.

Conclusions: Higher frequency of lesion occurrence in clinically eloquent WM tracts can characterize CIS subjects with different types of onset. The involvement of specific WM tracts, in particular those traversed by fibers involved in motor function and near the corpus callosum, seems to be associated with a higher risk of clinical conversion to MS in the short term. *Neurology*® 2013;80:234–241

Correspondence to Dr. De Stefano: destefano@unisi.it

GLOSSARY

ATR = anterior thalamic radiation; **CC** = corpus callosum; **CDMS** = clinically definite multiple sclerosis; **CIS** = clinically isolated syndrome; **CR** = corona radiata; **FLIRT** = FMRIB's linear image registration tool; **FMRIB** = Oxford Centre for Functional MRI of the Brain; **FSL** = FMRIB Software Library; **LPM** = lesion probability map; **LPMi** = lesion probability map index; **LV** = lesion volume; **MAGNIMS** = Magnetic Resonance in Multiple Sclerosis; **MNI** = Montreal Neurological Institute; **MS** = multiple sclerosis; **PD** = proton density; **SLF** = superior longitudinal fascicle; **T1-W** = T1-weighted; **T2-W** = T2-weighted; **WM** = white matter.

At disease onset, patients with clinically isolated syndrome (CIS) suggestive of multiple sclerosis (MS) have variable symptoms and brain white matter (WM) lesion loads.[1] Although the risk of conversion of CIS patients to clinically definite MS (CDMS) is related to the presence of brain WM lesions,[2–6] it is still unclear whether the specific anatomical location of these lesions has clinical implications.

MRI-derived spatial maps of brain lesions (lesion probability maps [LPMs]) have been used in previous works to assess differences across MS populations in probabilistic terms.[7–15] LPM evaluates in vivo the anatomical distribution and frequency of brain lesions and, by pooling information from

Editorial, page 230

Supplemental data at www.neurology.org

Supplemental Data

From the Department of Neurological and Behavioral Sciences (A.G., M.B., A.D.L, N.D.S.), University of Siena, Siena; Neuroimaging Research Unit (M.A.R., M.A., M.F.), Institute of Experimental Neurology, Division of Neuroscience, San Raffaele Scientific Institute, Vita-Salute San Raffaele University, Milan, Italy; Department of Radiology (R.v.S., F.B.), VU University Medical Centre, Amsterdam, the Netherlands; Department of Radiology and Neuroimmunology Unit (A.R., M.T), Hospital Vall d'Hebron, Barcelona, Spain; Departments of Neuroinflammation (D.C.) and Brain Repair and Rehabilitation (O.C.), University College London (UCL) Institute of Neurology, UCL, London, UK; Department of Neurology and Section of Neuroradiology (C.E.), Medical University of Graz, Graz, Austria; Neurology Unit (C.G.), San Camillo-Forlanini Hospital, Rome, Italy; and Department of Neurology (J.F.), Glostrup Hospital and University of Copenhagen, Denmark.

The current work was conducted on behalf of the MAGNIMS Study Group. Contributors who provided patient data and discussed the contents and interpretation of the study are listed on the *Neurology*® Web site at www.neurology.org.

Go to Neurology.org for full disclosures. Funding information and disclosures deemed relevant by the authors, if any, are provided at the end of the article.

MRI datasets, allows the visualization of spatial patterns of focal pathology that would be much less evident in single-patient studies.

Classic neuropathologic and MRI studies[16–18] have highlighted that MS lesions tend to have a predilection for certain areas of the brain, such as periventricular regions and corpus callosum (CC). However, lesions can be widespread across the brain even at disease onset, and, in this context, it would be very useful to know whether CIS patients with specific brain lesion distribution and frequency carry a high risk for early conversion to CDMS.

In this study, we used LPMs to assess, in a large population of patients with CIS, differences at baseline in brain lesion distribution and frequency a) between CIS patients with different types of clinical onset (optic neuritis, multifocal, brainstem/cerebellar, spinal cord, and cerebral hemispheric), and b) between patients who converted or did not convert to CDMS within 1 year.

METHODS

Study population. In this European, multicenter, retrospective study, we collected data of patients with CIS (n = 1165) from MS centers (Barcelona, Copenhagen, Graz, London, Milan, Rome, and Siena; n = 428 [36.7%]) and clinical trials on patients with CIS [19–21] (n = 737 [63.3%]). The study was organized and developed within the Magnetic Resonance in Multiple Sclerosis (MAGNIMS) network (www.magnims.eu). Clinical-demographic data were age, sex, date, topography of CIS, and date of conversion to CDMS due to a second clinical attack within 1 year from onset.

Standard protocol approvals, registrations, and patient consents. The study received approval from the local ethics committees and written informed consent was obtained from all study patients.

MRI data and analysis. MRI data were collected 60 ± 43 days from disease onset. Each participating center provided, for each patient, T1-weighted (T1-W), proton density (PD), and T2-weighted (T2-W) MRIs and T2-lesion masks, which were created in each center by using semiautomated segmentation techniques based on user-supervised local thresholding. All MRI data were sent to the Quantitative Neuroimaging Laboratory of the University of Siena for quality control and centralized T2 LPM analysis.

LPMs were obtained by using imaging analysis tools of the Oxford Centre for Functional MRI of the Brain (FMRIB) Software Library (FSL) (www.fmrib.ox.ac.uk/fsl/).[22] For each group studied here, the LPMs were created as follows:

1. The brain was first extracted from the T1-W, T2-W, and PD images using BET[22] and then a study-specific template was obtained after linearly registering a sample of T1-W brain images (n = 450, with equal numbers of images from the different magnetic resonance datasets) to the Montreal Neurological Institute (MNI)152 standard brain by using FMRIB's linear image registration tool (FLIRT)[22] and then averaging all the resulting transformed images.
2. A 2-stage registration was then performed to align the T2-lesion masks of each patient to the template. First, each lesion mask was linearly registered with FLIRT on the T1-W image using the transformation parameters derived by registering the PD on the T1-W image. Second, each lesion mask previously registered on the T1-W image was nonlinearly registered on the template with FMRIB's nonlinear image registration tool[23,24] using the transformation parameters derived by registering the T1-W image on the template. The nearest neighbor interpolation method was used in both stages. Two observers (A.G. and A.D.L.) independently checked all the coregistered lesion masks and an agreement was found in all cases.
3. For each patient group, an LPM was generated by first merging and then averaging all the standard-space lesion masks. For each map, voxel intensity represents the frequency of lesion occurrence in that voxel or, in other words, the probability of that voxel being lesion.

General statistics. To test for differences in age and lesion volume (LV) 1) between each type of onset and the remaining CIS population, and 2) between converting and nonconverting patients in the whole CIS population, and in each type of onset, nonparametric Mann-Whitney test was used. To account for differences in head size, for each patient LV was measured in common standard space, and this was used in all subsequent analyses.

Using the LPM, we computed a measure of the consistency of lesion pattern across patients of each group. This was described as the LPM index (LPMi) in a previous work[10] and was obtained by performing the following equation:

$$\mathrm{LPMi} = 100 \times [\mu(\mathrm{Mi} \times \mathrm{LPM_G})]$$

in which $\mathrm{LPM_G}$, the LPM of the patient group, was masked by Mi, the binarized and segmented lesion mask of the patient, and finally μ, the resulting mean inside the patient's mask, was computed. As a result of this procedure, LPMi is higher when the patient's lesion mask is localized in brain regions with a high probability of being lesion for that group. Differences in LPMi between converting and nonconverting patients in the whole CIS population were also assessed with Mann-Whitney test. The Fisher test was used for between-group comparisons of sex. Differences were considered significant at $p < 0.05$. Analyses were performed with the SPSS version 17 software (SPSS Inc., Cary, NC).

Voxelwise statistics. To test for between-group differences in lesion frequency, we performed unpaired *t* tests in a General Linear Model framework using *randomise,* a nonparametric permutation-based (n = 5,000 permutations) FSL program.[25] Moreover, analysis of variance was performed to test for significant heterogeneity in lesion frequency among the 5 CIS presentations. In all analyses, age, sex, slice thickness (3 mm [n = 1,001, 86%] and 5 mm [n = 164, 14%]), and the center creating lesion masks were included as covariates. In addition, because some studies[9,12,13] found that brain LV can influence lesion distribution, LPM analyses showing significant clusters were repeated after controlling for brain LV, which was log-transformed in order to obtain a normal distribution. Thresholding was performed using TFCE (Threshold-Free Cluster Enhancement), a method for finding significant clusters in MRI data without having to define them in a binary way.[26] Clusters were considered significant at $p < 0.05$, fully corrected for multiple comparisons across space.

Anatomical locations of the local maxima within significant clusters were determined using the diffusion tensor imaging and probabilistic tractography WM atlases included with FSL.

RESULTS Demographic, clinical, and MRI features of CIS patients are summarized in table 1. Conversion to CDMS occurred in 303 of 1,165 patients (26%) within 1 year from the first clinical event.

When compared with the remaining population, a greater LV was found in CIS patients with hemispheric (7.6 ± 8.3 cm^3 vs 4.9 ± 7 cm^3, $p < 0.001$) and multifocal (7.1 ± 10.1 cm^3 vs 4.7 ± 6.1 cm^3, $p < 0.001$) onset. Conversely, smaller LV was found, in comparison with the remaining CIS population, in patients with onset in the spinal cord (3.8 ± 5.4 cm^3 vs 5.5 ± 7.5 cm^3, $p < 0.001$) and optic nerve (3.8 ± 5 cm^3 vs 5.8 ± 7.9 cm^3, $p < 0.001$). Patients with brainstem/cerebellar onset had similar brain LV compared with the remaining CIS population (5.2 ± 6.1 cm^3 vs 5.2 ± 7.4 cm^3, $p > 0.10$).

In the whole population, there were no differences in age and sex ($p > 0.10$) between CIS patients who converted and those who did not convert to CDMS within 1 year. However, on the baseline MRI scans, LV of the CIS group converting within 1 year was greater than in the nonconverting group (7 ± 8.1 cm^3 vs 4.6 ± 6.7 cm^3, $p < 0.001$).

Similarly, when CIS patients were divided into different subgroups according to the type of onset, no differences in age and sex ($p > 0.10$) were found between converting and nonconverting patients (table 1). However, baseline LV was greater in the converting than in the nonconverting group in patients with brainstem/cerebellar, multifocal ($p \leq 0.001$ for both), optic nerve ($p = 0.01$), spinal cord ($p = 0.08$), and hemispheric ($p = 0.10$) onset (table 1).

LPM in patients grouped for disease onset. We assessed lesion distribution and frequency in CIS patients with different disease onset in comparison with the remaining population.

The LPM of CIS patients with hemispheric onset, compared with that of the remaining CIS population, showed higher ($p < 0.05$, cluster-corrected) lesion frequency in regions of the cerebral hemispheres such as the posterior and superior corona radiata (CR) mapping on the corticospinal tract and in the superior longitudinal fascicle (SLF). The clusters remained significant even after controlling for LV (figure 1, top panel).

In patients with multifocal onset, when compared with the remaining CIS population, a higher ($p < 0.05$, cluster-corrected) lesion frequency was found in several clusters of the cerebral WM. After controlling for brain LV, clusters in the SLF, anterior thalamic radiation (ATR), anterior CR mapping on the uncinate fascicle, and WM of the precentral gyrus were retained (figure 1, middle panel).

CIS patients with brainstem/cerebellar onset, compared with the remaining CIS population, showed higher ($p < 0.05$, cluster-corrected) lesion frequency, even after controlling for brain LV, in the middle cerebellar peduncle (figure 1, bottom panel).

By contrast, CIS patients with both optic nerve and spinal cord onset had lower ($p < 0.05$, cluster-corrected) lesion frequency than the remaining CIS population in several regions of the WM. However, none of these clusters survived correction for LV.

Overall, the anatomical location of significant clusters for the different types of CIS presentation was

Table 1 Clinical-demographic and MRI features of the patients with CIS

	Total CIS population (n = 1,165)	1-Year converting (n = 303)	Nonconverting (n = 862)
Age, y	31.2 ± 7.6	30 ± 7.2	31.6 ± 7.7
No. female/male (%)	793/372 (68/32)	216/87 (71.3/28.7)	577/285 (67/33)
Onset, n (%)	ON, 350 (30)	ON, 86 (28.5)	ON, 264 (30.6)
	MF, 246 (21)	MF, 71 (23.4)	MF, 175 (20.3)
	B/C, 218 (18.8)	B/C, 50 (16.5)	B/C, 168 (19.5)
	SC, 218 (18.8)	SC, 60 (19.8)	SC, 158 (18.3)
	CH, 133 (11.4)	CH, 36 (11.8)	CH, 97 (11.3)
T2-LV, cm^3	All onsets: 5.2 ± 7.2	All onsets: 7 ± 8.1	All onsets: 4.6 ± 6.7
	ON: 3.8 ± 5.0	ON: 4.7 ± 5.6	ON: 3.5 ± 4.8
	MF: 7.1 ± 10.1	MF: 9.1 ± 10.2	MF: 6.3 ± 9.9
	B/C: 5.2 ± 6.1	B/C: 8.7 ± 8.6	B/C: 4.1 ± 4.7
	SC: 3.8 ± 5.4	SC: 5 ± 7.3	SC: 3.3 ± 4.4
	CH: 7.6 ± 8.3	CH: 8.9 ± 8.9	CH: 7.1 ± 8.1

Abbreviations: B/C = brainstem/cerebellar; CH = cerebral hemispheric; CIS = clinically isolated syndrome; LV = lesion volume; MF = multifocal; ON = optic neuritis; SC = spinal cord.

Figure 1 Regions with high lesion frequency in clinically isolated syndrome patients with hemispheric, multifocal, and brainstem/cerebellar onset

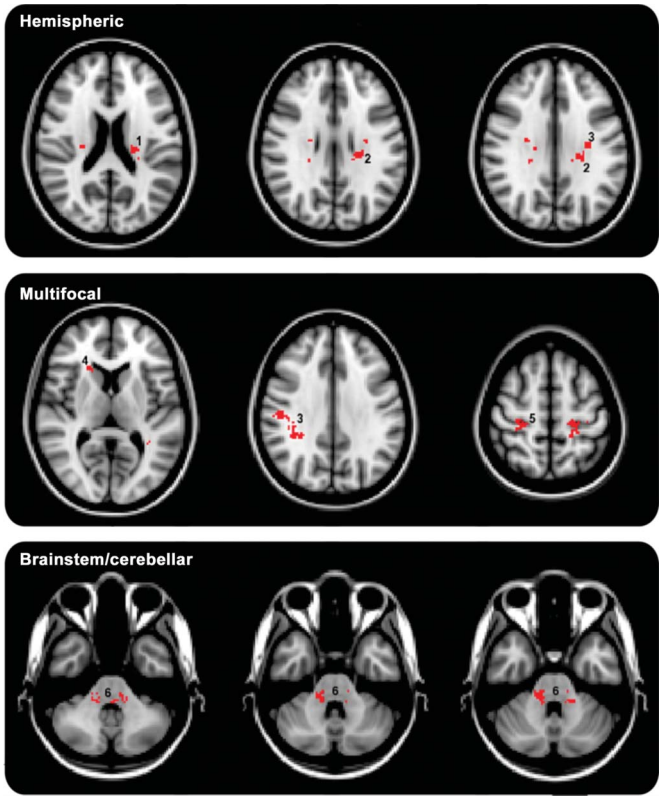

Red shows the clusters of voxels where, compared with the remaining clinically isolated syndrome population and after controlling for age, sex, slice thickness, center creating lesion masks, and brain lesion volume, there was higher ($p < 0.05$, cluster-corrected) frequency of lesion occurrence in patients with hemispheric (upper panel, n = 133), multifocal (middle panel, n = 246), and brainstem/cerebellar (bottom panel, n = 218) onset. Numbers represent the following white matter (WM) regions: 1) superior corona radiata; 2) posterior corona radiata; 3) superior longitudinal fascicle; 4) anterior thalamic radiation; 5) WM of the precentral gyrus; and 6) middle cerebellar peduncle. Background image is the Montreal Neurological Institute (MNI)152 standard space image. Images are shown in radiologic convention. See text for further details.

confirmed when an analysis of covariance was performed on the 5 CIS subgroups.

LPM in 1-year converting vs nonconverting CIS. The MRI-derived LPM of CIS patients who converted or did not convert within 1 year showed that lesions had an overall similar distribution across the brain (figure 2). However, in the converting group, baseline lesions tended to be more concentrated despite their greater volume, relatively sparing peripheral areas of the WM (figure 2). Indeed, the percentage of brain voxels occupied by lesions was 18% in the converting group and 25% in the nonconverting group. Moreover, the LPMi, which is a measure of the consistency of lesion pattern across patients of a group, was higher in converting than in nonconverting patients (3.5% ± 1.2% vs 2.2% ± 1.1%, $p < 0.001$).

The converting group had higher ($p < 0.05$, cluster-corrected) lesion frequency than the nonconverting group in projection, association, and commissural WM tracts (figure 3; table 2), with larger clusters (>40 voxels) in the CC (splenium, body, and genu), optic radiations, inferior frontooccipital fascicle, CR (anterior and superior regions), and cingulum. After controlling for LV, 2 clusters, 1 in the anterior CR mapping on the ATR and the other in the frontal cingulum, were retained (figure 3).

When the subgroups with different disease onset were considered in this voxelwise analysis, CIS patients with brainstem/cerebellar onset showed higher ($p < 0.05$, cluster-corrected) frequency of lesions in the converting group than in the nonconverting group, with clusters surviving correction for brain LV in the body of the CC, posterior CR mapping on the posterior part of the ATR and SLF. In patients with spinal cord onset, the converting group had higher ($p < 0.05$, cluster-corrected) lesion frequency than the nonconverting group in the region of the superior CR mapping on the corticospinal tract and in the SLF, all surviving correction for brain LV. By contrast, no difference in lesion frequency was found between converting and nonconverting groups in CIS subjects with hemispheric, multifocal, and optic nerve onset.

DISCUSSION It is well known from previous studies[2–6] that in CIS patients, the presence of a greater WM lesion load conveys a higher risk of developing CDMS. Less clear is whether or not CIS patients with different types of onset have different distribution of these cerebral lesions and, more importantly, whether the anatomical location of these lesions can predict an early conversion to CDMS. In this very large, retrospective, and multicenter study, we determined whether it is possible to provide an answer to these important questions by exploiting the potential of the MRI-derived LPMs in providing information that cannot be obtained with traditional MRI studies.

In CIS patients with different types of onset, the voxelwise analysis showed significant clusters of lesions in specific regions of the WM in patients with hemispheric (CR and SLF) and brainstem/cerebellar (middle cerebellar peduncle) onset. Clusters of lesions were found in several regions of the cerebral WM in patients with multifocal onset. Finally, significant lesion clusters were not found in patients with optic nerve and spinal cord onset. Altogether, these findings indicate a clear relationship between the type of clinical onset and the anatomical location of brain lesions, which goes well beyond what could emerge from single-patient studies.

It is potentially very important to recognize in advance CIS patients who will convert to CDMS in the short term, because this may have treatment implications. Patients with greater lesion load or fulfilling the Barkhof MRI criteria for disease dissemination in space,[27] compared with those who do not, are more likely to have a second episode.[4] In a recent study,[28] the combined presence of Barkhof criteria and lesions

Figure 2 T2-lesion probability maps in patients converting and not converting to clinically definite multiple sclerosis (MS) within 1 year

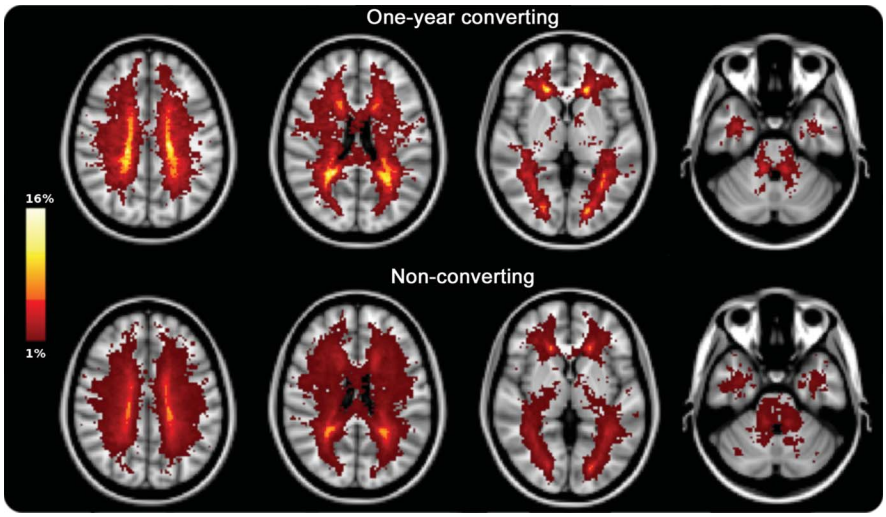

Upper and lower panels show, respectively, T2-lesion probability maps in standard space in patients converting (n = 303) and not converting (n = 862) to clinically definite MS within 1 year. The color overlay created on top of the Montreal Neurological Institute standard brain shows the probability of each voxel containing a lesion in each patient group. The color bar denotes the probability range. The percentage of brain voxels occupied by lesions was 18% in the converting group and 25% in the nonconverting group. The maximum local probability for lesions was 16% for the converted group in the region of the posterior corona radiata mapping on the corticospinal tract and 10% for the nonconverted group in the body of the corpus callosum. Images are shown in radiologic convention. See text for further details.

in the CC predicted conversion to CDMS, suggesting that the anatomical location of lesions is clinically relevant. The 2010 revisions to the McDonald criteria,[29] which incorporated the simplified MAGNIMS criteria for dissemination in space,[30] also highlight the importance of lesion topography for diagnosing MS. Our study adds to previous work by demonstrating that CIS patients who converted to CDMS within 1 year, compared with those who did not, show a higher probability of having lesions in projection, association, and commissural tracts of the WM. More specifically, the analysis identified the largest significant clusters in the CC, optic radiations, inferior frontooccipital fascicle, CR, and cingulum. Interestingly, in a recent study comparing, 20 years after clinical onset, the LPMs of patients with CDMS vs those who were still non-CDMS, lesions were also found to cluster in most of these WM regions.[8] Altogether, these studies imply that lesions occurring in regions traversed by fibers mediating motor and sensory functions are associated with a higher risk of further clinical episodes in the short term.

Among the lesion clusters identified in our work, those surviving LV correction were a region of the anterior CR located in the periventricular area of the frontal horn of the lateral ventricles and mapping on the ATR and the frontal cingulum, close to the rostral cingulate motor area. Both of them are clinically relevant regions of the frontal WM: the ATR is a WM projection tract that connects, through the anterior limb of the internal capsule, the frontal motor cortical areas, including premotor and supplementary motor areas, with the basal ganglia and brainstem nuclei; the cingulum is an important WM long association tract that runs parallel to the CC, connecting different parts of the cingulate gyrus with each other as well as with premotor regions, prefrontal cortex, parietotemporal lobes, basal ganglia, and motor nuclei of the brainstem. Notably, both anterior CR and cingulum are adjacent to the CC, which highlights once again the important role of callosal/pericallosal lesions in predicting future clinical attacks in patients with CIS.[28]

Voxel-based studies such as those performed here have strengths and limitations. Strength lies in the ability to study very large clinical and MRI datasets, as we have done here, and distill key information efficiently. LPM provides insights into the role of lesion location and distribution in predicting conversion from CIS to CDMS that would be difficult to achieve with manual or automated regional lesion counts. The very large dataset used here was made possible by the MAGNIMS network, which provided an amount of high-quality magnetic resonance data that could have never been collected in a single-center study. Moreover, some technical steps are also worthy of mention as potential strong points of this study: the use of nonlinear registration for creation of LPM allows alignment of patients' brains with great accuracy, diminishing the potential bias from errors in registration; the voxelwise analyses were based on nonparametric permutation testing, which is applicable even when the assumptions of a parametric approach

Figure 3 Regions with high lesion frequency in clinically isolated syndrome patients converting to clinically definite multiple sclerosis (MS) within 1 year

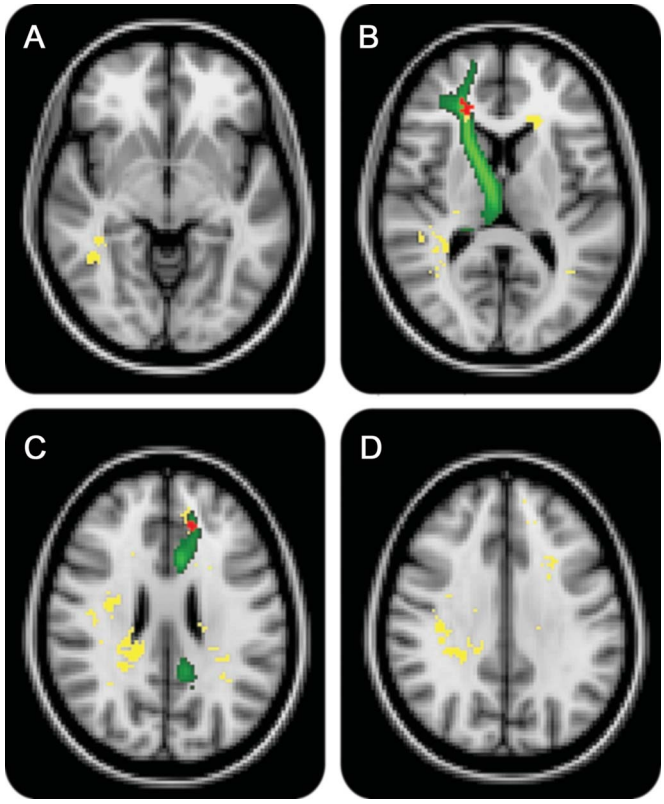

Yellow (in A-D) shows the clusters of voxels (see table 2) where, after controlling for age, sex, center, and slice thickness, brain lesions were more frequent ($p < 0.05$, cluster-corrected) in patients converting (n = 303) than in those not converting (n = 862) to clinically definite MS within 1 year. Red shows the clusters of voxels that also survived correction for lesion volume (anterior corona radiata in B and cingulum in C). Green represents the white matter fiber tracts (anterior thalamic radiation in B and cingulum in C) obtained from the FMRIB Software Library probabilistic tractography atlas. Background image is the Montreal Neurological Institute (MNI)152 standard space image. Images are shown in radiologic convention. See text for further details.

Table 2 Regions of the WM where, in the whole population of CIS patients, lesion frequency of the 1-year converting group (n = 303) was higher ($p < 0.05$, cluster-corrected) than in the nonconverting group (n = 862)

WM region (local maxima)	Side	MNI (mm) X	Y	Z	t Statistic
PCR mapping on the CST	R	22	−32	34	4.8
	L	−22	−24	24	4.5
OR	L	−32	−44	16	4.8
Splenium of the CC	R	18	−38	26	4.6
IFOF	R	38	−46	−4	4.4
ILF	L	−36	−62	4	4.3
SCR mapping on the SLF	L	−22	12	30	4.2
ATR	R	18	18	20	4.1
WM of middle frontal gyrus	R	34	8	48	4.1
ACR mapping on the ATR	R	22	34	8	4.0
ACR mapping on the forceps minor	L	−18	30	14	4.0
Anterior cingulum	L	−14	36	26	4.0
Genu of the CC mapping on the forceps minor	L	−16	30	8	3.6
Body of the CC	R	18	−12	34	3.2
WM of postcentral gyrus	R	34	−26	50	3.1
WM of precentral gyrus	R	14	−24	44	3.0

Abbreviations: ACR = anterior corona radiata; ATR = anterior thalamic radiation; CC = corpus callosum; CIS = clinically isolated syndrome; CST = corticospinal tract; IFOF = inferior frontooccipital fascicle; ILF = inferior longitudinal fascicle; MNI = Montreal Neurological Institute; OR = optic radiation; PCR = posterior corona radiata; SCR = superior corona radiata; SLF = superior longitudinal fascicle; WM = white matter.

are not valid, as in the case of study groups with different numbers of subjects[25]; and the use of correction for multiple comparisons across space for all voxelwise analyses, thus reducing the risk of false-positive results.

The study also has a number of limitations. First is the short-term clinical follow-up of our CIS population, because longer follow-up times could have provided more clinically meaningful results. However, although short-term prediction of clinical conversion to MS is not informative about long-term prognosis, it can still be very important for treatment decisions in CIS subjects.[19–21,31–33] Second, there was a greater LV in the converting than in the nonconverting patients, which could have biased the interpretation of our LPM results. Including LV as a covariate in the statistical model may yield spurious results because regional and whole brain lesion loads tend to covary, and it is for this reason that several recent studies have chosen not to include it in the statistical models or to present both LV-corrected and noncorrected results.[7–15,34–38] Reassuringly, in this study, we provided results both with and without correction for LV, obtaining similar overall results. Third, data from different centers have been acquired with different sequence geometry. Nevertheless, the use of nonlinear registration and the correction of all voxelwise analyses for slice thickness and center creating lesion masks should not have affected the overall anatomical distribution and location of the brain lesions. Finally, we also have to consider that some CIS patients had received disease-modifying treatment after the first clinical episode and that the clinical assessment schedule differed between the different clinical trials.

Overall, our study using MRI-derived LPM in a very large patient population after the first clinical event

suggestive of MS implies that there are regional differences in lesion frequency in clinically eloquent WM tracts that can differentiate CIS subjects with different types of presentation. Moreover, projection, association, and commissural tracts of the WM, in particular those traversed by fibers involved in motor function and close to the CC (i.e., anterior CR and cingulum), are associated with a higher risk of further clinical episodes in the short term.

AUTHOR CONTRIBUTIONS

Antonio Giorgio: study concept and design, acquisition of data, analysis and interpretation, critical revision of the manuscript for important intellectual content. Marco Battaglini: analysis and interpretation, critical revision of the manuscript for important intellectual content. Maria Assunta Rocca: acquisition of data, critical revision of the manuscript for important intellectual content. Alessandro De Leucio, Martina Absinta, Ronald van Schijndel, Alex Rovira, Mar Tintoré, Declan Chard, Olga Ciccarelli, Christian Enzinger, Claudio Gasperini, and Jette Frederiksen: acquisition of data, critical revision of the manuscript for important intellectual content. Massimo Filippi and Frederik Barkhof: critical revision of the manuscript for important intellectual content. Nicola De Stefano: study concept and design, analysis and interpretation, critical revision of the manuscript for important intellectual content, study supervision.

ACKNOWLEDGMENT

The authors thank Bayer HealthCare Pharmaceuticals, Merck Serono, and Teva Pharmaceutical Industries for authorizing the use of trial data.

STUDY FUNDING

No targeted funding reported.

DISCLOSURE

A. Giorgio and M. Battaglini report no disclosures. M.A. Rocca serves as consultant to Bayer Schering Pharma, received speakers' bureaus for Biogen-Dompé, and receives research support from the Italian Ministry of Health. A. De Leucio, M. Absinta, and R. van Schijndel report no disclosures. A. Rovina serves on scientific advisory boards for NeuroTEC, Bayer Schering Pharma, and BTG International Ltd., has received speaker honoraria from Bayer Schering Pharma, Sanofi-Aventis, Stendhal, Bracco, Merck Serono, Teva Pharmaceutical Industries Ltd., and Biogen Idec, receives research support from Bayer Schering Pharma, and serves as a consultant for Novartis. M. Tintoré has received compensation for consulting services and speaking from Bayer Schering, Merck Serono, Biogen-Idec, Teva, Sanofi-Aventis, and Novartis. D. Chard receives research support from the Multiple Sclerosis Society of Great Britain and Northern Ireland and holds stock in GlaxoSmithKline. O. Ciccarelli receives research grant support from the Multiple Sclerosis Society of Great Britain and Northern Ireland and from the Department of Health Comprehensive Biomedical Centre; she has received honoraria from Bayer Schering and GE. C. Enzinger has received travel grants and speaking honoraria from Biogen-Idec, Teva-Aventis, Merck Serono, Bayer Schering, and unrestricted research grants from Teva-Aventis and Merck Serono. C. Gasperini has received speaker honoraria from Bayer Schering Pharma, Sanofi-Aventis, Merck Serono, Biogen Idec, and Novartis J. Frederiksen reports no disclosures. M. Filippi serves on scientific advisory boards for Teva Pharmaceutical Industries Ltd. and Genmab A/S; has received funding for travel from Bayer Schering Pharma, Biogen-Dompé, Genmab A/S, Merck Serono, and Teva Pharmaceutical Industries Ltd.; serves as a consultant to Bayer Schering Pharma, Biogen-Dompé, Genmab A/S, Merck Serono, and Teva Pharmaceutical Industries Ltd.; serves on speakers' bureaus for Bayer Schering Pharma, Biogen-Dompé, Genmab A/S, Merck Serono, and Teva Pharmaceutical Industries Ltd.; and receives research support from Bayer Schering Pharma, Biogen-Dompé, Genmab A/S, Merck Serono, Teva Pharmaceutical Industries Ltd., and Fondazione Italiana Sclerosi Multipla. F. Barkhof works in consultancy with Bayer Schering Pharma, Sanofi-Aventis, Biogen-Idec, UCB, Merck Serono, Novartis, Roche, Synthon BV, Janes Research, and Lundbeck; he receives honoraria for consultancy above; he receives a grant from the Dutch MS Society; he receives payment for development of educational presentations including service on speakers' bureaus from the Serono Symposia Foundation. N. De Stefano serves on scientific advisory boards for Merck Serono; has received funding for travel from Teva Pharmaceutical Industries Ltd. and Merck Serono; has received speaker honoraria from Teva Pharmaceutical Industries Ltd., BioMS Medical, Biogen Idec, Bayer Schering Pharma, and Merck Serono. Go to Neurology.org for full disclosures.

Received May 29, 2012. Accepted in final form August 31, 2012.

REFERENCES

1. Miller DH, Chard DT, Ciccarelli O. Clinically isolated syndromes. Lancet Neurol 2012;11:157–169.
2. Optic Neuritis Study Group. Multiple sclerosis risk after optic neuritis: final optic neuritis treatment trial follow-up. Arch Neurol 2008;65:727–732.
3. Fisniku LK, Brex PA, Altmann DR, et al. Disability and T2 MRI lesions: a 20-year follow-up of patients with relapse onset of multiple sclerosis. Brain 2008;131:808–817.
4. Tintoré M, Rovira A, Rio J, et al. Baseline MRI predicts future attacks and disability in clinically isolated syndromes. Neurology 2006;67:968–972.
5. Ruet A, Deloire MS, Ouallet JC, et al. Predictive factors for multiple sclerosis in patients with clinically isolated spinal cord syndrome. Mult Scler 2011;17:312–318.
6. Minneboo A, Barkhof F, Polman CH, et al. Infratentorial lesions predict long-term disability in patients with initial findings suggestive of multiple sclerosis. Arch Neurol 2004;61:217–221.
7. Narayanan S, Fu L, Pioro E, et al. Imaging of axonal damage in multiple sclerosis: spatial distribution of magnetic resonance imaging lesions. Ann Neurol 1997;41:385–391.
8. Dalton C, Bodini B, Samson R, et al. Brain lesion location and clinical status 20 years after a diagnosis of clinically isolated syndrome suggestive of multiple sclerosis. Mult Scler 2012;18:322–328.
9. Kincses ZT, Ropele S, Jenkinson M, et al. Lesion probability mapping to explain clinical deficits and cognitive performance in multiple sclerosis. Mult Scler 2011;17:681–689.
10. Di Perri C, Battaglini M, Stromillo ML, et al. Voxel-based assessment of differences in damage and distribution of white matter lesions between patients with primary progressive and relapsing-remitting multiple sclerosis. Arch Neurol 2008;65:236–243.
11. Bodini B, Battaglini M, De Stefano N, et al. T2 lesion location really matters: a 10 year follow-up study in primary progressive multiple sclerosis. J Neurol Neurosurg Psychiatry 2011;82:72–77.
12. Vellinga MM, Geurts JJ, Rostrup E, et al. Clinical correlations of brain lesion distribution in multiple sclerosis. J Magn Reson Imaging 2009;29:768–773.
13. Sombekke MH, Vellinga MM, Uitdehaag BM, et al. Genetic correlations of brain lesion distribution in multiple sclerosis: an exploratory study. AJNR Am J Neuroradiol 2011;32:695–703.
14. Charil A, Zijdenbos AP, Taylor J, et al. Statistical mapping analysis of lesion location and neurological disability in multiple sclerosis: application to 452 patient data sets. Neuroimage 2003;19:532–544.

15. Ceccarelli A, Rocca MA, Pagani E, et al. The topographical distribution of tissue injury in benign MS: a 3T multiparametric MRI study. Neuroimage 2008;39:1499–1509.
16. Miller DH, Albert PS, Barkhof F, et al. Guidelines for the use of magnetic resonance techniques in monitoring the treatment of multiple sclerosis. US National MS Society Task Force. Ann Neurol 1996;39:6–16.
17. Brownell B, Hughes JT. The distribution of plaques in the cerebrum in multiple sclerosis. J Neurol Neurosurg Psychiatry 1962;25:315–320.
18. Lucchinetti CF, Bruck W, Rodriguez M, Lassmann H. Distinct patterns of multiple sclerosis pathology indicates heterogeneity on pathogenesis. Brain Pathol 1996;6:259–274.
19. Kappos L, Polman CH, Freedman MS, et al. Treatment with interferon beta-1b delays conversion to clinically definite and McDonald MS in patients with clinically isolated syndromes. Neurology 2006;67:1242–1249.
20. Comi G, Filippi M, Barkhof F, et al. Effect of early interferon treatment on conversion to definite multiple sclerosis: a randomised study. Lancet 2001;357:1576–1582.
21. Comi G, Martinelli V, Rodegher M, et al. Effect of glatiramer acetate on conversion to clinically definite multiple sclerosis in patients with clinically isolated syndrome (PreCISe study): a randomised, double-blind, placebo-controlled trial. Lancet 2009;374:1503–1511.
22. Smith SM, Jenkinson M, Woolrich MW, et al. Advances in functional and structural MR image analysis and implementation as FSL. Neuroimage 2004;23(suppl 1):S208–S219.
23. Andersson JLR, Jenkinson M, Smith S. Non-linear optimisation. FMRIB technical report TR07JA1. Available at: www.fmrib.ox.ac.uk/analysis/techrep. 2007. Accessed November 27, 2012.
24. Andersson JLR, Jenkinson M, Smith S. Non-linear registration, aka Spatial normalisation. FMRIB technical report TR07JA2. Available at: www.fmrib.ox.ac.uk/analysis/techrep. 2007. Accessed November 27, 2012.
25. Nichols TE, Holmes AP. Nonparametric permutation tests for functional neuroimaging: a primer with examples. Hum Brain Mapp 2002;15:1–25.
26. Smith SM, Nichols TE. Threshold-free cluster enhancement: addressing problems of smoothing, threshold dependence and localisation in cluster inference. Neuroimage 2009;44:83–98.
27. Barkhof F, Filippi M, Miller DH, et al. Comparison of MRI criteria at first presentation to predict conversion to clinically definite multiple sclerosis. Brain 1997;120(pt 11):2059–2069.
28. Jafari N, Kreft KL, Flach HZ, et al. Callosal lesion predicts future attacks after clinically isolated syndrome. Neurology 2009;73:1837–1841.
29. Polman CH, Reingold SC, Banwell B, et al. Diagnostic criteria for multiple sclerosis: 2010 revisions to the McDonald criteria. Ann Neurol 2011;69:292–302.
30. Montalban X, Tintoré M, Swanton J, et al. MRI criteria for MS in patients with clinically isolated syndromes. Neurology 2010;74:427–434.
31. Jacobs LD, Beck RW, Simon JH, et al. Intramuscular interferon beta-1a therapy initiated during a first demyelinating event in multiple sclerosis. CHAMPS Study Group. N Engl J Med 2000;343:898–904.
32. Kappos L, Freedman MS, Polman CH, et al. Effect of early versus delayed interferon beta-1b treatment on disability after a first clinical event suggestive of multiple sclerosis: a 3-year follow-up analysis of the BENEFIT study. Lancet 2007;370:389–397.
33. Kappos L, Freedman MS, Polman CH, et al. Long-term effect of early treatment with interferon beta-1b after a first clinical event suggestive of multiple sclerosis: 5-year active treatment extension of the phase 3 BENEFIT trial. Lancet Neurol 2009;8:987–997.
34. Reuter F, Zaaraoui W, Crespy L, et al. Cognitive impairment at the onset of multiple sclerosis: relationship to lesion location. Mult Scler 2011;17:755–758.
35. Calabrese M, Battaglini M, Giorgio A, et al. Imaging distribution and frequency of cortical lesions in patients with multiple sclerosis. Neurology 2010;75:1234–1240.
36. Sepulcre J, Masdeu JC, Pastor MA, et al. Brain pathways of verbal working memory: a lesion-function correlation study. Neuroimage 2009;47:773–778.
37. Sepulcre J, Masdeu JC, Sastre-Garriga J, et al. Mapping the brain pathways of declarative verbal memory: evidence from white matter lesions in the living human brain. Neuroimage 2008;42:1237–1243.
38. Lee MA, Smith S, Palace J, et al. Spatial mapping of T2 and gadolinium-enhancing T1 lesion volumes in multiple sclerosis: evidence for distinct mechanisms of lesion genesis? Brain 1999;122(pt 7):1261–1270.